Ann. Geophys., 26, 1189–1197, 2008
www.ann-geophys.net/26/1189/2008/

Annales Geophysicae

Long-term trends in the ionospheric E and F1 regions

J. Bremer

Leibniz-Institute of Atmospheric Physics, 18225 Kühlungsborn, Schloss-Str. 6, Germany

Received: 10 May 2007 – Revised: 13 November 2007 – Accepted: 13 November 2007 – Published: 28 May 2008

Abstract. Ground based ionosonde measurements are the most essential source of information about long-term variations in the ionospheric E and F1 regions. Data of such observations have been derived at many different ionospheric stations all over the world some for more than 50 years. The standard parameters *foE*, *h'E*, and *foF1* are used for trend analyses in this paper. Two main problems have to be considered in these analyses. Firstly, the data series have to be homogeneous, i.e. the observations should not be disturbed by artificial steps due to technical reasons or changes in the evaluation algorithm. Secondly, the strong solar and geomagnetic influences upon the ionospheric data have carefully to be removed by an appropriate regression analysis. Otherwise the small trends in the different ionospheric parameters cannot be detected.

The trends derived at individual stations differ markedly, however their dependence on geographic or geomagnetic latitude is only small. Nevertheless, the mean global trends estimated from the trends at the different stations show some general behaviour (positive trends in *foE* and *foF1*, negative trend in *h'E*) which can at least qualitatively be explained by an increasing atmospheric greenhouse effect (increase of CO_2 content and other greenhouse gases) and decreasing ozone values. The positive *foE* trend is also in qualitative agreement with rocket mass spectrometer observations of ion densities in the E region. First indications could be found that the changing ozone trend at mid-latitudes (before about 1979, between 1979 until 1995, and after about 1995) modifies the estimated mean *foE* trend.

Keywords. Atmospheric composition and structure (Ion chemistry of the atmosphere; Thermosphere-composition and chemistry) – Ionosphere (Ionosphere-atmosphere interactions; Solar radiation and cosmic ray effects) – Radio science (Ionospheric propagation; Remote sensing)

Correspondence to: J. Bremer
(bremer@iap-kborn.de)

1 Introduction

Trend analyses with ionospheric data have mainly been initiated by model results of Roble and Dickinson (1989) assuming a doubling of the atmospheric greenhouse gases CO_2 and CH_4 in the Earth's atmosphere. Based on these results Rishbeth (1990) and Rishbeth and Roble (1992) predicted a lowering of the F2-layer by about 15–20 km and of the E-layer by about 2.5 km. Additionally they prognosticated a decrease of the peak electron density of the F2-layer (decrease of foF2 by about 0.2–0.5 MHz) and an increase of the peak electron density of the F1- and E-layers (*foF1* increase by about 0.3–0.5 MHz; *foE* increase by 0.05–0.08 MHz). During the following years a lot of investigations have been carried out to test these predictions using ionosonde observations at different stations. Most of these investigations deal, however, with trends in the ionospheric F2-layer (peak height, i.e. hmF2, as well as peak electron density expressed by foF2). A compilation of these results can be found in Bremer (2005). Trend analyses with ionosonde parameters of the E- and F1-layer are fewer and mostly restricted to one or a few stations (Bremer, 1992; Givishvilli et al., 1995; Sharma et al., 1999). Only some papers deal with the results of more globally distributed stations (Bremer, 1998, 2001, 2004; Mikhailov and de la Morena, 2003; Bremer et al., 2004; Mikhailov, 2006).

In this present paper earlier results of trend analyses with characteristic ionosonde parameters of the ionospheric E- and F1-regions (Bremer, 1998; 2001; 2004) will be updated using data series newly extended to the year 2005. New aspects of this paper deal with latitudinal and longitudinal variations of the ionospheric trends as well as the influence of ozone variations on these trends.

2 Data analysis and methodical investigations

In the trend analyses presented here monthly median values of the following characteristic ionosonde parameters of the E- and F1-region are used: *foE* , *h'E*, and *foF1*. In Fig. 1 one example of such data series is shown. Here the local noon

Published by Copernicus Publications on behalf of the European Geosciences Union.

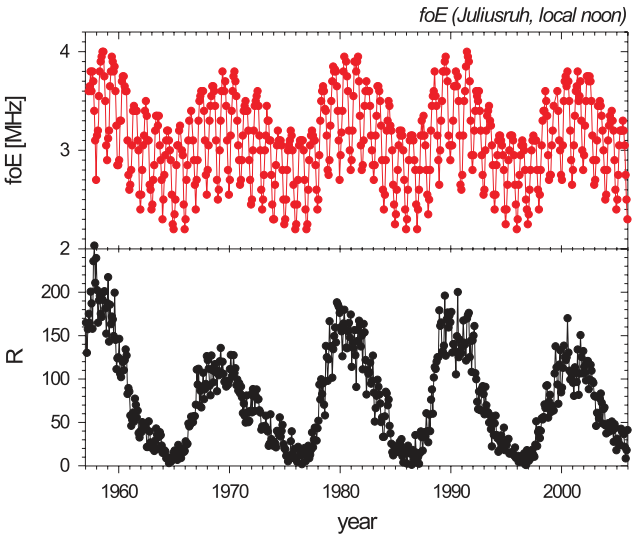

Fig. 1. Long-term variations of monthly mean *foE* values of the ionosonde station Juliusruh at local noon (upper part) and of solar sunspot number *R* (lower part).

foE values of the station Juliusruh (54.6° N; 13.4° E) are presented (upper part) together with the solar sunspot number R (lower part). Two things can obviously be remarked, firstly the *foE* values are markedly dependent on the solar activity and secondly the *foE* values have a pronounced seasonal variation. Moreover, *foE* has also a diurnal variation, not to be seen in Fig. 1 because it is restricted to a fixed time (local noon). This variability has to be taken into consideration in the trend analyses. Therefore, the elimination of the solar and geomagnetic influences upon the observed parameters $X_{\rm obs}$=*foE*, *h'E* or *foF1* are carried out for each hour and each month separately. At first the solar and geomagnetically induced parts of the ionospheric parameter are estimated by the following twofold regression formula

$$X_{th} = a + b \cdot R + c \cdot Ap. \quad (1)$$

Here R is the solar sunspot number as proxy of the solar activity, Ap is the global geomagnetic activity index, b and c are the corresponding partial regression coefficients, and a is constant factor describing X_{th} for R=0 and Ap=0. Then the difference between the observed and calculated ionospheric parameters are estimated by

$$\Delta X = X_{\rm obs} - X_{th} \quad (2)$$

or the relative differences are calculated

$$\Delta X = (X_{\rm obs} - X_{th}) \big/ X_{th}. \quad (3)$$

Trend analyses can be done for each hour and each month separately, but often the ΔX data series are combined to get more representative yearly mean ΔX values which are also used in this paper to derive linear trends according to

$$\Delta X = d + e \cdot \text{year}. \quad (4)$$

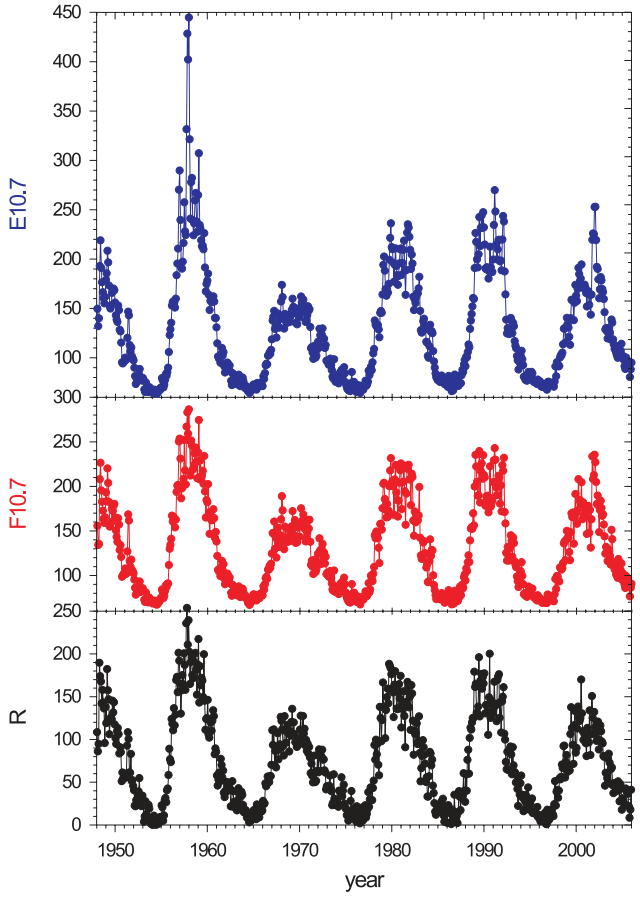

Fig. 2. Long-term variations of different solar activity indices: solar sunspot number *R*, solar 10.7 cm radio flux F10.7, and solar EUV proxy E10.7.

Here the value e is the trend parameter for the individual station whereas d is a constant factor for ΔX at year=0.

In Eq. (1) the solar sunspot number is used as the solar activity index. It is however also possible to use other indices as the solar 10.7 cm radio flux F10.7 or the EUV proxy E10.7 (Tobiska, 2001). In Fig. 2 these three indices are presented for the time period between 1948 and 2005. In spite of some unusually high monthly mean values of the E10.7 index during 1957 all three indices are very strongly correlated (e.g. correlation coefficients $r(R, \text{F10.7})$=0.975, $r(R, \text{E10.7})$=0.948). Therefore, the choice of the solar activity index should not be very critical.

In Fig. 3 the results of trend analyses with *foE*, *h'E* and *foF1* data series from observations at Juliusruh are presented using different solar indices. For strong trends (here in *h'E*) the choice of the solar index is totally uncritical. For very small and insignificant trends (here mainly in *foF1*) the derived trends may however slightly differ in dependence on the used solar activity index. Therefore, in trend analyses of different stations always the same index should be used. In agreement with earlier investigations by the author the solar sunspot number *R* is used in this present analysis.

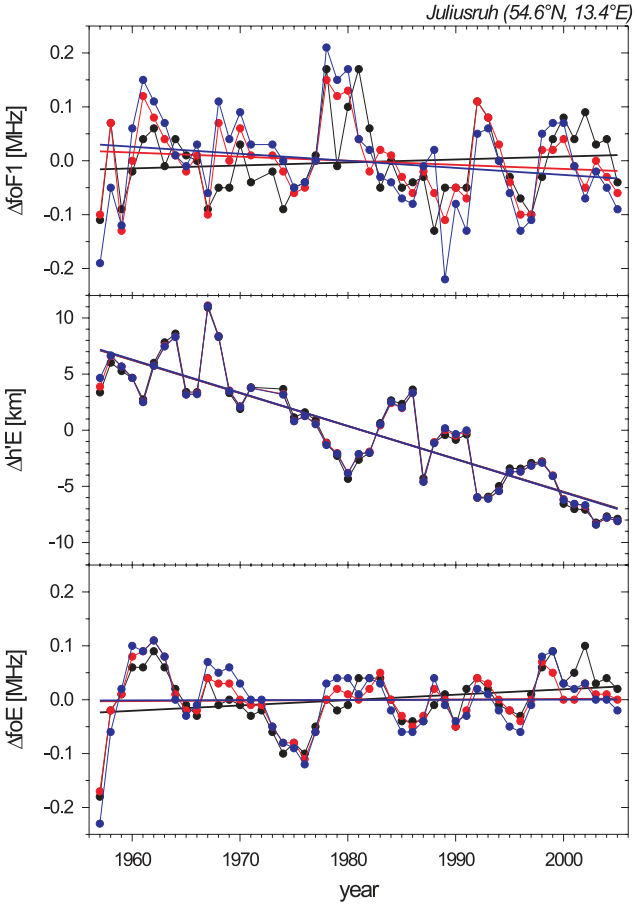

Fig. 3. Long-term trends of different ionospheric parameters (*foE*, *h'E*, *foF1*) observed at the ionosonde station Juliusruh after elimination of the solar and geomagnetic influences using different solar activity indices (R: black, F10.7: red, E10.7: blue).

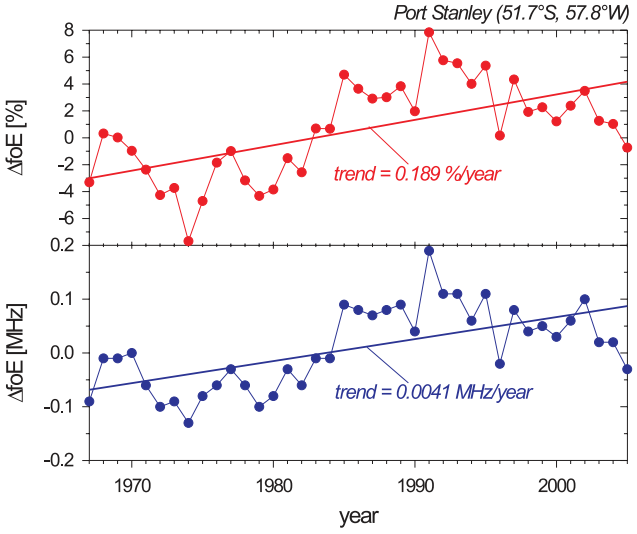

Fig. 4. Trends in *foE* of the ionosonde station Port Stanley derived from absolute (lower part) and relative differences (upper part) between experimental and regression model values.

As mentioned above the trend analyses can be made with absolute (Eq. 2) or relative differences (Eq. 3). In Fig. 4 one example is shown with *foE* trends derived from ionosonde observations at the station Port Stanley (51.7° S, 57.8° W) using both methods. The long-term variations of the derived ΔfoE values are very similar and the derived linear trends are nearly identical if we use a mean *foE* value of 2.2 MHz. Therefore, also the choice of both methods seems to be uncritical. In this present paper absolute differences according to Eq. (2) are used in agreement with earlier papers of the author.

3 Experimental trends from global ionosonde observations

In the following the results of the trend analyses are presented for the different characteristic ionospheric parameters separately. In each case only yearly ΔX data series have been investigated to get most reliable data series. These data series have been derived from all ΔX data series for each month and each hour where observation data are available, i.e. without night-time values for *foE*, *h'E*, and *foF1* as well as without winter values for *foF1*. Also other missing data (e.g. caused by technical reasons) have not been included in the analyses, e.g. by use of interpolation methods. The length of the individual data series is different reaching from 15 years up to 49 years. The first year of the analysed data is 1957 as in connection with the International Geophysical Year (IGY) a lot of ionosondes started their operation in this year, the last analysed year is 2005.

3.1 Trends in *foE*

From 71 different globally distributed ionosonde stations individual *foE* trends have been derived. In Fig. 5 these individual trends are shown in a histogram (right part). Negative values are in red, positive values in blue. The significant trends are in dark colours (confidence level greater than 95%), the non-significant trends (confidence level less than 95%) in light colours. The significance of the individual trends has been tested by the Fisher's F parameter

$$F = r^2 \cdot (n-2) \Big/ (1-r^2). \quad (5)$$

Here r is the correlation coefficient between ΔX and year after Eq. (4) and n is the number of years with data. The significance levels for the F parameter can be found in Taubenheim (1969). The median value of the individual trends (marked by the arrow in the histogram) is 0.0011 MHz/year.

In the left part of Fig. 5 the mean global *foE* trend is estimated from all 71 individual ΔfoE data series. The derived mean global trend is 0.0013 MHz/year. The corresponding

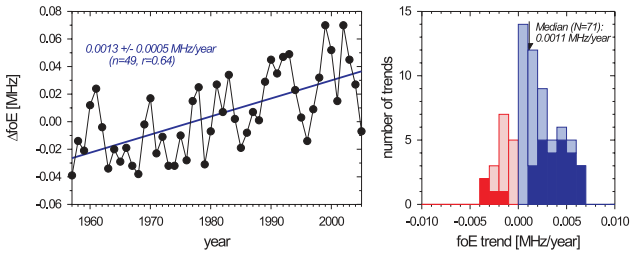

Fig. 5. Global mean *foE* trend (left part) and histogram (right part) deduced from observations at 71 individual ionosonde stations.

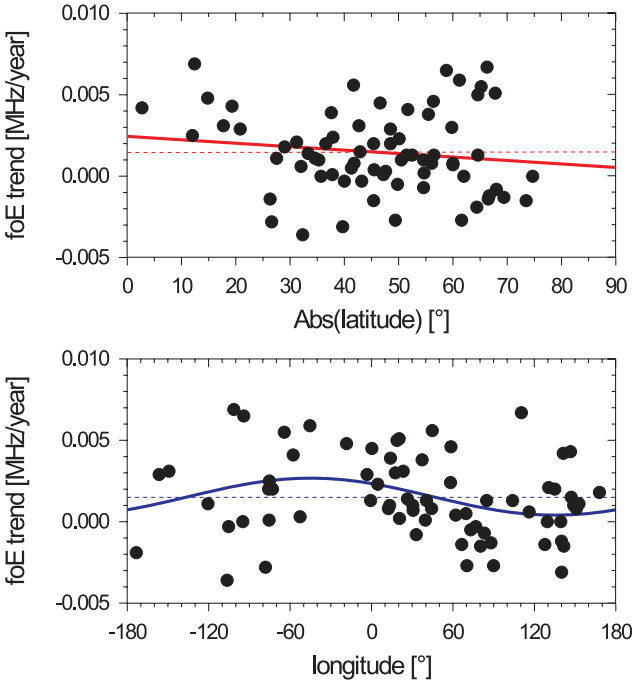

Fig. 6. *foE* trends in dependence on the absolute value of the latitude of the individual stations (upper part) and on the longitude of these stations (lower part). The dashed lines characterize the mean global *foE* trend, the full lines are the curves of the best linear fit (upper part) and sinusoidal fit (lower part) through the individual trend values.

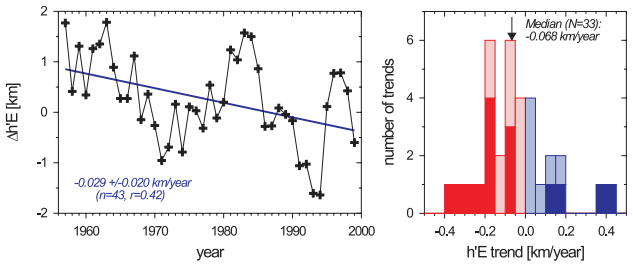

Fig. 7. Global mean *h'E* trend (left part) and histogram (right part) deduced from observations at 33 individual ionosonde stations.

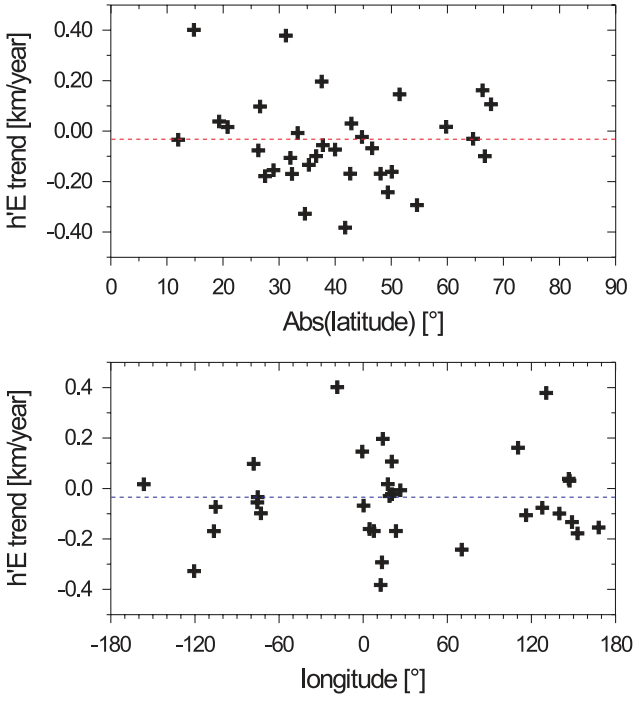

Fig. 8. *h'E* trends in dependence on the absolute value of the latitude of the individual stations (upper part) and on the longitude of these stations (lower part). The dashed lines characterize the mean global *h'E* trend.

error of this trend has been calculated with the following formula (Taubenheim, 1969)

$$\text{Error}(95\%) = t_\beta(n-2) \Big/ \sqrt{(n-2)} \cdot \sqrt{s_x^2 \Big/ s_y^2 - e^2_{\Delta x(y)}}. \quad (6)$$

Here t_β is the threshold value of the Student's t test with a confidence level of 95%, n the number of years, s_x^2 and s_y^2 are the variances of X (=*foE*, *foF1*, or *h'E*) and of y (=year), and e is the regression coefficient (= trend value) from Eq. (4). For X=*foE* the estimated mean error is ±0.0005 MHz/year. Therefore, the mean global *foE* trend is significantly different from zero. Inside of the left part of Fig. 5 the trend value with error limits is presented including the number n of years used in the mean trend analysis and the correlation coefficient r between Δ*foE* and year. Using these values the corresponding F parameter according to Eq. (5) can easily be estimated (F=47.9) which demonstrates a strongly significant correlation between Δ*foE* and year (confidence level above 99%) thus confirming the result presented above by use of Eq. (6). The derived mean trend in the left part of Fig. 5 agrees reasonably with the median value of the individual trends in the right part.

In Fig. 6 the individual *foE* trends are presented in dependence on the absolute value of the latitude of the stations (upper part) and in dependence on the longitude (lower part). The dashed lines represent the mean *foE* trend. There is an indication that the *foE* trends may slightly be stronger at low

latitudes, however the slope of the estimated linear regression line (full red line in the upper part of Fig. 6) is not significant (confidence level only about 50% due to Fisher's F parameter test). The individual *foE* trends in dependence on latitude have been fitted by a sinusoidal curve (full blue curve in the lower part of Fig. 6). Here a tendency of a small latitudinal variation of the *foE* trends can be seen with a maximum near 40° W and a minimum near 140° E. In spite of the strong variability of the individual trends this result is however an indication of a latitudinal dependence of *foE* trends. The correlation between the individual trend values and the corresponding values from the fitted curve (r=0.36) is significant with a confidence level of about 99%.

3.2 Trends in *h'E*

Trends in the virtual height of the ionospheric E layer, *h'E*, have been derived from data series of 33 different ionosonde stations. These individual trends are presented in a histogram (right part of Fig. 7). Negative trends are in red, positive in blue. Significant trends are marked by dark colours, non-significant trends by light colours. The median value is −0.068 km/year.

In the left part of Fig. 7 the mean global *h'E* trend is shown calculated from all 33 individual Δ*h'E* data series. The mean trend is −0.029 km/year and therefore different from the median value of the individual trends in the right part of Fig. 7. The reason of this difference may be the small number of available stations and the strong differences between the individual trend values producing a relatively disturbed histogram with some peaks. In spite of the small number of available stations the mean trend is significant with more than 95% confidence as to be seen by the error which is markedly smaller than the mean trend (see numbers in the left part of Fig. 7). This result can be confirmed by the Fisher's F test. Using the correlation coefficient r and the number of years n as presented in the left part of Fig. 7, a value F=6.6 can be estimated due to Eq. (5) which demonstrates a significant correlation between Δ*h'E* and year with a confidence level of more than 95%.

The dependences of the *h'E* trends on the absolute value of the latitude and on the longitude of the individual ionosonde stations are presented in Fig. 8. There are no remarkable dependencies to be seen, probably caused by the limited number of available stations. The dashed lines mark the mean *h'E* trend as derived in the left part of Fig. 7.

3.3 Trends in *foF1*

Similar as above for *foE* and *h'E* the trend results for *foF1* observations are presented in Fig. 9. In the right part of Fig. 9 the histogram is presented for the individual *foF1* trends with a median value of 0.0021 MHz/year. The positive trends are presented in blue, the negative in red. The significant trends

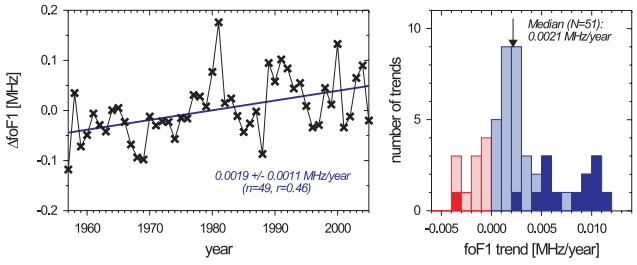

Fig. 9. Global mean *foF1* trend (left part) and histogram (right part) deduced from observations at 51 individual ionosonde stations.

are characterized by dark colours, the non-significant trends by light colours.

In the left part of Fig. 9 the mean global *foF1* trend is shown estimated from the Δ*foF1* data series of all 51 available stations. The mean trend with 0.0019 MHz/year agrees reasonably with the median value of all individual trends. As the error limit is markedly smaller than the mean value (see numbers inside the left part of Fig. 9), the derived global trend is significant with more than 95%. This fact can also be confirmed by the calculation of the F value according to Eq. (5) with the r and n values shown inside of the left part of Fig. 9. The estimated value F=12.6 indicates a significant correlation between Δ*foF1* and year with a confidence level of more than 99%.

In Fig. 10 the individual *foF1* trends are presented in dependence on the absolute values of the latitude as well as on the longitude of the available measuring stations. There seems to be a slight tendency that *foF1* trends at low latitudes become stronger similar as also observed in the upper part of Fig. 6 for *foE* trends. The derived slope of the linear regression line (full red line in the upper part of Fig. 11) is due to the Fisher's F parameter test significant with about 88% confidence. There is however no visible dependence of the *foF1* trends on the longitude (lower part of Fig. 10). The dashed lines in both parts of Fig. 10 mark the mean *foF1* trend as derived in the left part of Fig. 9.

3.4 Influence of ozone on trends in *foE*

From long-term observation of the total ozone content in the atmosphere over Europe (Krzyscin et al., 2005) periods with different ozone trends can be detected, only small trends before 1979, a marked decrease between 1979 and 1995, and a small ozone increase after about 1995. These features can also be seen in the total ozone data series observed at Arosa (coordinates: 46.8° N, 9.7° E; data source: Mäder, 2005, and DWD, 2005) in Fig. 11. After elimination of the solar and geomagnetically induced parts a mean total ozone trend has been derived with −0.44 DU/year for the full period between 1957 and 2005 (red line), whereas the trends in the above mentioned sub-intervals are quite different. We know from model results (Bremer and Berger, 2002;

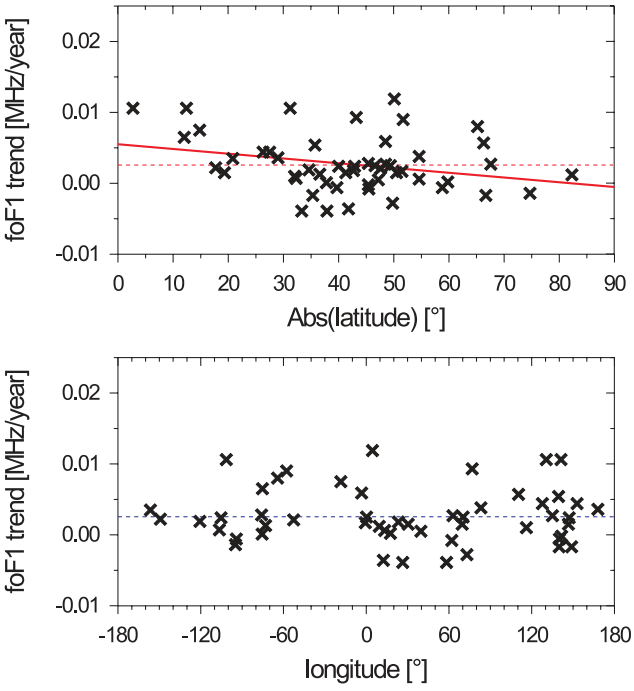

Fig. 10. *foF1* trends in dependence on the absolute value of the latitude of the individual stations (upper part) and on the longitude of these stations (lower part). The dashed lines characterize the mean global *foF1* trend, the full red line in the upper part is the best linear fit through the individual trend values.

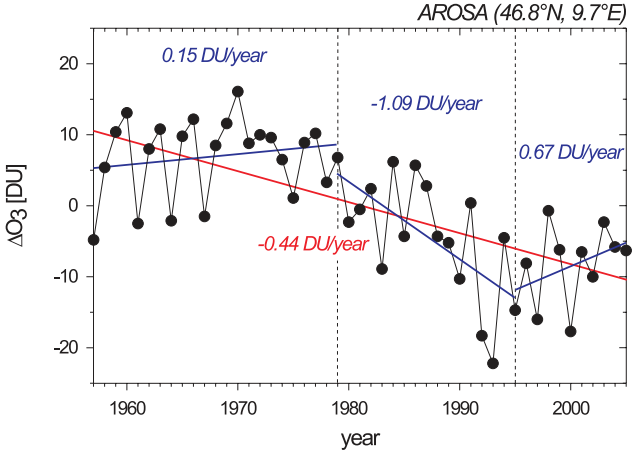

Fig. 11. Long-term variation of total ozone observed at Arosa after elimination of the solar and geomagnetic influences. The red line is the linear trend for the whole interval between 1957 and 2005, the blue lines characterize the trends in different sub-intervals.

Akmaev et al., 2006) that ozone changes may influence not only the stratosphere but also the meso- and lower thermosphere. Therefore, it seems to be reasonable to investigate whether the different ozone trends may influence trends in the E region. In Fig. 12 the variation of mean ΔfoE values

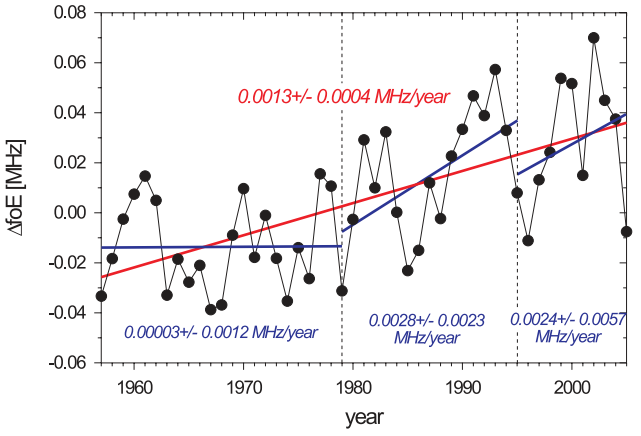

Fig. 12. Long-term variation of *foE* deduced from observations at 45 stations in mid-latitudes (30–60° N, 30–60° S) after elimination of the solar and geomagnetic influences. The red line is the linear trend for the whole interval between 1957 and 2005, the blue lines characterize the trends in different sub-intervals.

is shown, here however estimated only from 45 stations at mid-latitudes (30–60° S and 30–60° N). The mean trend (red line) is identical with the mean global *foE* trend shown in Fig. 5 (left part). Also the estimated error value is similar to the value for the global trend, thus confirming the high confidence level of this long-term trend. The *foE* trends in the three sub-intervals (blue lines) are quite different with a very small trend before 1979, a steep increase of the trend during the time period between 1979 and 1995, and a reduced trend after 1995. Due to the short length of these sub-intervals the estimated trends can describe only the main features of the ΔfoE variations and there remain some discrepancies between the trend values at the boundaries of adjacent intervals. The confidence levels of these trends are partly very small. Only for the second interval (1979–1995) the confidence level is markedly higher than 95%, for the third interval this level is only 64% whereas in the first interval the ΔfoE trend is nearly zero. Nevertheless there are some similarities between the ozone trends in Fig. 11 and the trends in *foE* in Fig. 12. This statement is confirmed by the correlation between ΔfoE values from Fig. 12 and ΔO_3 data from Fig. 11 presented in Fig. 13 with a significant correlation coefficient $r(\Delta foE, \Delta O_3)=-0.57$.

4 Discussion

To derive reasonable long-term trends from ionosonde data it is necessary to have homogeneous data series of sufficient length. In particular artificial steps due to technical changes or changes of the evaluation method may produce erroneous trends. Therefore, data series with such steps have been excluded from the trend analyses. The length of the observation period should be as large as possible. Here only data series

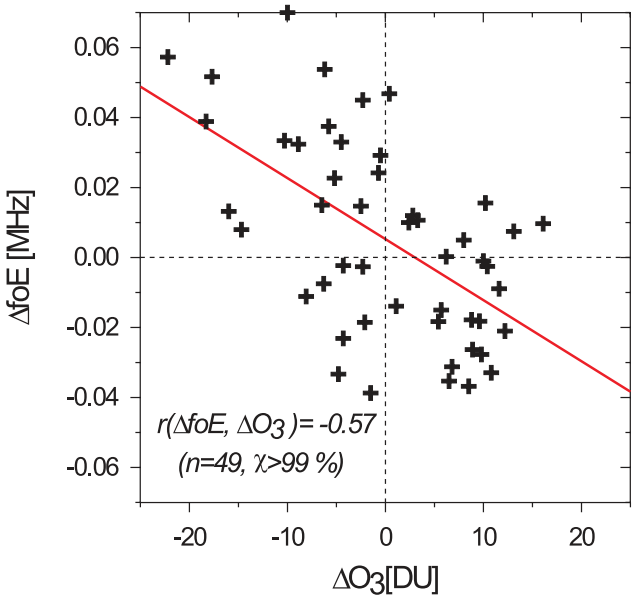

Fig. 13. Correlation between 49 yearly mean values of ΔfoE deduced from ionosonde observations at mid-latitudes and ΔO_3 at Arosa.

Table 1. Mean global trends in different ionospheric parameters. N is the number of ionosonde stations used in the trend analyses.

Region	Parameter	N	Mean exp. trend	Error (95%)
F1	*foF1*	51	0.0019 MHz/year	±0.0011 MHz/year
E	*foE*	71	0.0013 MHz/year	±0.0005 MHz/year
E	*h'E*	33	−0.029 km/year	±0.020 km/year

with more than 15 years have been used; most of the series are however longer than two solar cycles, extending to 49 years at maximum.

The method used to derive long-term trends has been described in Section 2 above. As demonstrated there the choice of the solar activity index as well as the method using absolute or relative differences between the observed and modelled data is uncritical and should not influence the presented trend results markedly. But there is another trend method developed by Mikhailov and de la Morena (2003) which uses quite another algorithm. These authors try to exclude long-term variations of the geomagnetic activity. Their results cannot directly be compared with the results presented in this paper. These authors believe that before about 1970 the long-term variation of *foE* is mainly controlled by the long-term variation of the geomagnetic activity, after that time, however, a *foE* increase should be caused by anthropogenic sources.

In spite of the exclusion of non-homogeneous data series the differences between individual trends in all ionospheric

Table 2. The experimental trends of different ionospheric parameters, their extrapolation to CO_2*2 conditions, and, for direct comparison, the model results of Rishbeth (1990) and Rishbeth and Roble (1992).

Parameter	Mean exp. Trend	CO_2*2 (exp)	CO_2*2 (mod)
foF1	0.0019 MHz/year	0.38 MHz	0.3...0.5 MHz
foE	0.0013 MHz/year	0.26 MHz	0.05...0.08 MHz
h'E	−0.029 km/year	−5.8 km	−2.5 km

parameters analysed here are relatively strong as can be seen in the histograms presented in the right parts of Figs. 5, 7, and 9. The reasons for these differences are not quite clear, some of them may be caused by their geographical locations. E.g. there are small indications that the *foE* and *foF1* trends are more pronounced at low latitudes than at mid- and high latitudes (see upper parts of Figs. 6 and 10), but the confidence levels of the corresponding regression lines are small as already remarked above in Sects. 3.1 and 3.3.

As there is no strong dependence of the detected trends in *foE*, *h'E* and *foF1* on latitude and longitude it seems to be reasonable to compare the globally averaged trends of these parameters with the model predictions of Rishbeth (1990) and Rishbeth and Roble (1992). In Table 1 the mean experimental trends are compiled together with their error bars. In contrast to these trends in MHz/year or km/year the model predictions in Table 2, CO_2*2 (mod), are given for a doubling of the greenhouse gases (mainly CO_2). For a comparison of both results it is necessary to look at the changes of these gases during the last 40 years. Due to Houghton et al. (2001) and Brasseur and de Rudder (1987) an effective increase of the greenhouse gases of about 20% can be assumed for the last 40 years. If we further assume a linear dependence between the content of greenhouse gases and the ionospheric trend effect then we can easily estimate from the derived experimental trends the expected ionospheric effect for a doubling of the greenhouse gases called CO_2*2 (exp). A comparison of the experimental trends with the model data in Table 2 gives for all three parameters the same sign but differences in the amplitudes of the trends. In the E region the mean experimental trend is markedly stronger than the model value. The agreement of the *foF1* trends is however surprisingly good. The observed *foE* increase is in qualitative agreement with a negative trend in the ion ratio $[NO^+]/[O_2^+]$ as detected by Danilov and Smirnova (1997) with rocket borne mass spectrometer measurements at E region heights. This negative trend should decrease the effective recombination coefficient as the recombination coefficient of NO^+ is markedly larger than that of O_2^+, and therefore an increasing electron density can be expected. A negative trend in the ion ratio $[NO^+]/[O_2^+]$ should be caused by

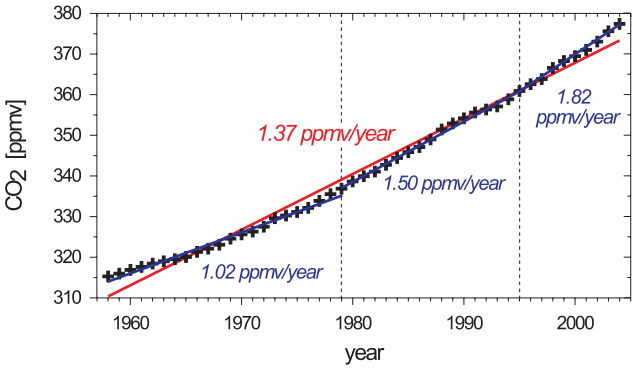

Fig. 14. Long-term variation of CO_2 observed at Hawaii. The red line is the linear trend for the whole interval between 1958 and 2004, the blue lines characterize the trends in different sub-intervals.

the reduced NO density as predicted from model calculations for an increasing greenhouse effect (Roble and Dickinson, 1989; Beig, 2000).

One reason for the observed discrepancies between observed and modelled data in the E region may result from the fact that in the model calculations of Roble and Dickinson (1989), Rishbeth (1990) and Rishbeth and Roble (1992) only the trends of the greenhouse gases CO_2 and CH_4 have been considered. But also ozone (Bremer and Berger, 2002; Akmaev et al., 2006) as well as water vapour trends (Akmaev et al., 2006) can amplify the modelled trends.

The influence of ozone trends on the *foE* trends is demonstrated in Figs. 11–13 above. The dates of possible trend changes have mainly been derived from long-term ozone changes (Krzyscin et al., 2005). The year 1979 is also supported by stratospheric trend analyses of Labitzke and Naujokat (2000) with clearly changing temperature trends at this time. The *foE* trends in the different sub-intervals in Fig. 12 are of course not only caused by the changing ozone trends but also by the CO_2 trends. In Fig. 14 the long-term variation of CO_2 is presented derived from observations at Hawaii (Keeling and Whorf, 2005). Due to these measurements the CO_2 trend increases steadily from the interval before 1979 with 1.03 ppmv/year until 1.82 ppmv/year, to the interval after 1995. Therefore, for the explanation of the *foE* trends the influence of different greenhouse gases (CO_2, CH_4, O_3, H_2O and others) have to be taken into account. Here it should only be expressed that in agreement with model results (Akmaev et al., 2006) ozone changes influences also long-term trends in the E region. In the global *h'E* trend the influence of ozone could, however, not be detected, probably due to the markedly reduced data volume (only data from 33 stations and not enough data after 1999).

In the F1 region no influence of ozone changes upon *foF1* trends have been found. Here the influence ozone should also be markedly smaller than in the E region as derived by Akmaev et al. (2006) in their model calculations.

It is not quite clear if the latitudinal variation of the *foE* trends in the lower part of Fig. 6 is a real effect or only an artefact. However, the possibility cannot be excluded that the individual trends may depend on their latitude. In solar cycle effects of the temperature in the strato- and mesosphere some zonal asymmetric effects have been found (Hampson et al., 2006). Therefore, in the future this effect has to be investigated in more detail, e.g. for different seasons.

5 Summary and conclusions

Using data series from long-term observations at globally distributed ionosonde stations, the trends of different characteristic ionospheric parameters (*foE*, *h'E*, *foF1*) have been derived. The main results can be summarized as follows:

- The detection of relatively small long-term trends in ionospheric data series requires the careful elimination of the strong solar and geomagnetic influences as always mentioned by the author in previous publications and also found by a lot of other investigators. Here a twofold regression analysis is made using different solar activity indices and the global geomagnetic Ap index.
- The globally averaged mean trends (positive trends in *foE* and *foF1*, negative *h'E* trend) qualitatively agree with model calculations of the effect of the increasing atmospheric greenhouse effect. However, the experimental trends in the E region are markedly stronger than in the model predictions.
- The derived trends at the individual stations differ markedly. There are some indications of a slight latitudinal dependency (stronger trends at lower latitudes in *foE* and *foF1*), however the confidence level is relatively low. The *foE* trend values slightly depend on the longitude with an indication of a simple sinusoidal variation.
- Changes in the mid-latitude total ozone trends modify the *foE* trends. Therefore, stratospheric ozone changes also influence long-term variations in the lower thermosphere in qualitative agreement with model results. The extension of the ionospheric data series until 2005 was very helpful for these investigations.
- General remark: In trend analyses it should carefully be checked whether the investigated time interval can be analysed by a simple linear regression line (or another continuous curve) or whether it is more reliable to subdivide the interval into different sub-periods, especially if there are physical reasons to do it.

Acknowledgements. The author is very grateful to the reviewers A. D. Danilov and M. J. Jarvis for their critical and very helpful remarks and comments to this paper.

Topical Editor M. Pinnock thanks A. Danilov, M. Jarvis, and another anonymous referee for their help in evaluating this paper.

References

Akmaev, R. A., Fomichev, V. I., and Zhu, X.: Impact of middle-atmospheric composition changes on greenhouse cooling in the upper atmosphere, J. Atmos. Sol.-Terr. Phy., 68, 1879–1889, doi:10.1016/j.jastp.2006.03.008, 2006.

Beig, G.: The relative importance of solar activity and anthropogenic influences on the ion composition, temperature, and associated neutrals of the middle atmosphere, J. Geophys. Res., 105, 19 841–19 856, 2000.

Brasseur, G. and de Rudder, A.: The potential impact on atmospheric ozone and temperature of increasing trace gas concentrations, J. Geophys. Res., 92, 10 903–10 920, 1987.

Bremer, J.: Ionospheric trends in mid-latitudes as a possible indicator of the atmospheric greenhouse effect, J. Atmos. Terr. Phy., 54, 1505–1511, 1992.

Bremer, J.: Trends in the ionospheric E and F regions over Europe, Ann. Geophys., 16, 986–996, 1998, http://www.ann-geophys.net/16/986/1998/.

Bremer, J.: Trends in the thermosphere derived from global ionosonde observations, Adv. Space Res., 28(7), 997–1006, 2001.

Bremer, J.: Investigations of long-term trends in the ionosphere with world-wide ionosonde observations, Adv. Radio Sci., 2, 253–258, 2004, http://www.adv-radio-sci.net/2/253/2004/.

Bremer, J.: Long-term trends in different ionospheric layers, Radio Sci. Bulletin, 315, 22–32, 2005.

Bremer, J., Alfonsi, L., Bencze, P., Lastovicka, J., Mikhailov, A. V., and Rogers, N.: Long-term trends in the ionosphere and upper atmosphere parameters, Ann. Geophys., Suppl. to 47, N 2/3, 1009–1029, 2004.

Bremer, J. and Berger, U.: Mesospheric temperature trends derived from ground-based LF phase-height observations at mid-latitudes: comparison with model simulations, J. Atmos. Sol.-Terr. Phy., 64, 805–816, 2002.

Danilov, A. D. and Smirnova, N. V.: Long-term trends in the ion composition of the E region (in Russian), Geomagn. Aeron., 37(5), 35–40, 1997.

DWD: Ozonbulletin des Deutschen Wetterdienstes, http://www.dwd.de/ozonzentrum, 2005.

Givishvilli, G. V., Leshchenko, N. L., Shmeleva, O. P., and Ivanidze, T. G.: Climatic trends of the mid-latitude upper atmosphere and ionosphere, J. Atmos. Terr. Phy., 57, 871–874, 1995.

Hampson, J., Keckhut, P., Hauchecorne, A., and Chanin, M. L.: The effect of the 11-year solar-cycle on the temperature in the upper-stratosphere and mesosphere - Part III: Investigations of the zonal asymmetry, J. Atmos Sol.-Terr. Phy., 68, 1591–1599, doi:10.1016/j.jastp.2006.05.006, 2006.

Houghton, J. D., Ding, Y., Griggs, D. J., Noguer, M., van der Linden, P. J., Dai, X., Maskell, K., and Johnson, C. A.: Climate Change: The Scientific Basis, Contribution of WG I to the 3rd Assessment Report of the IPCC, Cambridge, University Press, 2001.

Keeling, C. D. and Whorf, T. P.: Atmospheric CO_2 records from sites in the SIO air sampling network, in: Trends: A Compendium of Data on Global Change, Carbon Dioxide Information Analysis Center, Oak Ridge National Laboratory, U.S. Department of Energy, Oak Ridge, Tenn., USA, 2005.

Krzyscin, J. W., Jaruslawski, and Rajewska-Wiech, B.: Beginning of the ozone recovery over Europe?-Analysis of the total ozone data from the ground-based observations, 1964–2004, Ann. Geophys., 23, 1685–1695, 2005, http://www.ann-geophys.net/23/1685/2005/.

Labitzke, K. and Naujokat, B.: The lower arctic stratosphere in winter since1952, SPARC Newsletter No. 15, 11–14, 2000.

Mäder, J.: Total ozone series in Arosa, Switzerland, http://www.iac.ethz.ch/en/research/chemie/tpeter/totozon.html, 2005.

Mikhailov, A. V.: Trends in the ionospheric E-region, Phys. Chem. Earth, 31, 22–33, doi:10.1016/j.pce.2005.02.005, 2006.

Mikhailov, A. V. and de la Morena, B. A.: Long-term trends of foE and geomagnetic activity variations, Ann. Geophys., 21, 751–760, 2003, http://www.ann-geophys.net/21/751/2003/.

Roble, R. G. and Dickinson, R. E.: How will changes of carbon dioxide and methane modify the mean structure of the mesosphere and thermosphere?, Geophys. Res. Lett., 16, 1441–1444, 1989.

Rishbeth, H.: A greenhouse effect in the ionosphere?, Planet. Space Sci., 38, 945–948, 1990.

Rishbeth, H. and Roble, R. G.: Cooling of the upper atmosphere by enhanced greenhouse gases – Modelling of the thermospheric and ionospheric effects, Planet. Space Sci., 40, 1011–1026, 1992.

Sharma, S., Chandra, H., and Vyas, G. D.: Long term trends over Ahmedabad, Geophys. Res. Lett., 26, 433–436, 1999.

Taubenheim, J.: Statistische Auswertung geophysikalischer und meteorologischer Daten, Akad. Verlagsgesellschaft Geest & Portig K.-G., Leipzig, 1969.

Tobiska, W. K.: Validating the solar EUV proxy, E10.7, J. Geophys. Res., 106, 29 969–29 978, 2001.